astronomy

MDPI

Article

Towards the Particle Spectrum, Tickled by a Distant Massive Object

Mehdi Dehghani [1], Salman A. Nejad [2,*] and Maryam Mardaani [1]

[1] Department of Physics, Faculty of Science, Shahrekord University, Shahrekord 8818634141, Iran; dehghani@sku.ac.ir (M.D.); m64mardaani@gmail.com (M.M.)
[2] Department of Physical Sciences, Embry-Riddle Aeronautical University, Daytona Beach, FL 32114, USA
* Correspondence: abarghos@my.erau.edu

Abstract: To investigate the gravitational effects of massive objects on a typical observer, we studied the dynamics of a test particle following BMS_3 geodesics. We constructed the BMS_3 framework using the canonical phase space formalism and the corresponding Hamiltonian. We focused on analyzing these effects at fine scales of spacetime, which led us to quantization of the phase space. By deriving and studying the solutions of the quantum equations of motion for the test particle, we obtained its energy spectrum and explored the behavior of its wave function. These findings offer a fresh perspective on gravitational interactions in the context of quantum mechanics, providing an alternative approach to traditional quantum field theory analyses.

Keywords: BMS_3; first class constraints; canonical structure; quantum mechanics

check for updates

Citation: Dehghani, M.; A. Nejad, S.; Mardaani, M. Towards the Particle Spectrum, Tickled by a Distant Massive Object. *Astronomy* **2024**, *3*, 304–318. https://doi.org/10.3390/astronomy3040019

Academic Editor: Ignatios Antoniadis

Received: 12 October 2024
Revised: 21 November 2024
Accepted: 4 December 2024
Published: 12 December 2024

1. Introduction

The symmetries of spacetime seen by an observer located far away from all sources of gravitational field are given by the BMS group. By definition, the BMS group represents the asymptotic symmetries of "asymptotically flat" spacetimes at future null infinity. These spacetimes approach the Minkowski metric—a flat spacetime described by the metric of special relativity, characterized by its zero curvature and global Lorentz invariance—near the boundary of spacetime, which holds in regions far from heavy objects and without imposing additional assumptions about spacetime, such as specific topologies or the presence of a cosmological constant [1]. BMS group was introduced in 1962 by Bondi, van der Burg, Metzner, and Sachs to study the flow of energy at infinity of a propagating gravitational wave [2–4].

Before the discovery of the BMS group, the naive expectation for asymptotically flat spacetime symmetries was to extend and reproduce the symmetries of flat spacetime of special relativity via the Poincaré group, as a ten-dimensional group of three Lorentz boosts, three rotations, and four spacetime translations [5]. Being curious about the physically sensible boundary conditions to place on the gravitational field at light-like infinity, Bondi et al. found the asymptotic symmetry transformations form a group with a structure independent of any particular gravitational field present. This implies that at spatial infinity, it is possible to separate the kinematics of spacetime from the dynamics of the gravitational field [2], where general relativity does not reduce to special relativity in the case of weak fields at long distances [6].

The resulting symmetry group, known as the BMS group, is an infinite-dimensional extension of the finite-dimensional Poincaré group. While the Poincaré group, which is a subgroup of the BMS group, includes Lorentz transformations as asymptotic symmetries, the BMS group also introduces an infinite set of additional symmetries known as superrotations and supertranslations [4]. Since its inception, the BMS group has played a pivotal role in the study of quantum gravity [1] and has garnered significant attention in recent years, particularly in the context of the AdS/CFT correspondence and its application to flat-space holography [1,7–25].

The asymptotic symmetry groups of three-dimensional gravity have been studied by Brown and Henneaux [26]. In general n-dimensional spacetime, the symmetry algebra consists of the semi-direct sum of the conformal Killing vectors of a $(n-2)$-dimension sphere acting on the ideal of infinitesimal supertranslations [7,27].

Recently, the existence of unexplored degrees of freedom closely connected to the BMS group has been proposed [1]. Studying such degrees of freedom may open new windows to quantum gravity problems since the pure Einstein–Hilbert gravity in three dimensions exhibits no propagating physical degrees of freedom [28–31]. Those degrees of freedom may also account for the Bekenstein–Hawking entropy of realistic black holes in four dimensions [1]. In his 2015 talk, Hawking proposed that the information loss paradox can be resolved by considering the supertranslation of the horizon caused by the ingoing particles [32]. However, this is not all about those extra degrees of freedom. There is another way to look at them via the context of usual quantum mechanics. As we know, the Poincaré group plays an important role in the classification of particles according to their spin and mass. In Minkowski spacetime, in the absence of gravity, all the quantities form Poincaré representations, and this can be seen after the extraction of the quantum Dirac equation.

Properties of the Poincaré group and their connection to BMS algebra have motivated us to understand the group representations for particles. In this work, we aim to examine the possibility of extracting the spin state for the particle in this background after quantization is applied. In addition to its algebraic properties and the profound physical implications of this symmetry, the BMS space can be investigated from the perspective of a test particle and its phase space, which reveals and embodies the symmetric properties of the spacetime.

This research serves as the foundation for this exploration. A free particle, devoid of any external potential, is placed within this background, and we aim to quantize it by analyzing the particle's phase space to observe the effects of its presence in this space. In classical mechanics, a particle lives on geodesics, and after quantization, it will live on the quantized texture of spacetime. Thus, we interpret this work as the quantization of the geodesics of the BMS space.

From the classical perspective, a particle's trajectory is determined by geodesics, which can be derived using standard general relativity methods. In this study, we focus on the structure of this space—namely, its phase space, with the goal of quantizing it, which is equivalent to quantizing the BMS_3 geodesics. By investigating the quantized nature of this spacetime, we aim to examine properties such as the spectrum of a free particle inhabiting this space and to explore whether the spacetime reveals any additional physical insights about the particle.

To achieve this goal, the paper is organized as follows. In Section 2, we construct a quantized toy model in a $(2+1)$-dimensional framework, where a particle of mass m exists in the three-dimensional BMS space, referred to as BMS_3 thereafter. In Section 3, we formulate the corresponding Hamiltonian and study the phase space structure to develop a quantized model. This approach involves quantizing the classical geodesics along which the particle moves. Finally, we provide an initial analysis of the energy spectrum of the free particle and the behavior of its wave function.

2. Model Structure

Bondi coordinates are established from an outgoing light cone congruence, with its radial sections determined by the luminosity distance [33]. They are employed in the Bondi–Sachs formalism of general relativity, as a metric-based approach to solving the Einstein equations. This formalism uses coordinates tailored to the null geodesics of spacetime, or null rays, which represent the trajectories of gravitational waves. The analysis of the

Bondi–Sachs metric at infinity leads to the Bondi–Metzner–Sachs (BMS) group, a symmetry group present at null infinity [27,34].

In our analysis, we chose to work in the Bondi–Metzner–Sachs (BMS) coordinate system, as the BMS group serves as a natural extension of the Poincaré group. This choice is not arbitrary: the Poincaré-invariant action inherently preserves BMS invariance, making BMS coordinates particularly suitable for addressing the quantization problem.

The BMS_3 coordinates are defined via the set of retarded Bondi coordinates (r, φ, u),

$$r = \sqrt{x^2 + y^2}, \qquad re^{i\varphi} = x + iy, \qquad u = t - r, \tag{1}$$

where, as shown in Figure 1, $u \in \mathbb{R}$ is the time-like coordinate, aka retarded time, $r \in [0, +\infty)$ is the distance to the observer which is located in the origin of the $x - y$ plane, having the polar angle $\varphi \in \mathbb{R}$ according to the x coordinate with the identification $\varphi \sim \varphi + 2\pi$, forming a non-orthogonal curvilinear coordinates [16,35],

$$\hat{e}_r.\hat{e}_\varphi = 0, \qquad \hat{e}_u.\hat{e}_\varphi = 0, \qquad \hat{e}_r.\hat{e}_u = \frac{\sqrt{2}}{2}. \tag{2}$$

The third scalar product refers to the emergence of a Lagrangian constraint between u and r.

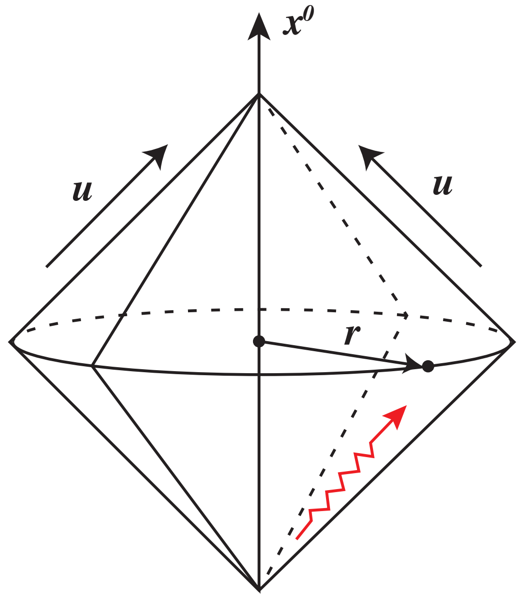

Figure 1. The coordinates u and r in spacetime are shown as in [1], with the time coordinate x^0 pointing upward. The wavy red line represents a massless particle emitted at $r = 0$ and traveling outward along a light cone generator ($u =$ const) to a non-zero r. The circle of radius r represents a sphere in four-dimensional spacetime.

In this coordinate system, the line element is rewritten as

$$ds^2 = -du^2 - 2dudr + r^2 d\varphi^2. \tag{3}$$

By its construction, coordinate u will play the role of time evolution parameter.

Let us consider a particle with the rest mass m, living in such a spacetime. The action of the model is the action of such a constrained particle, testing the BMS_3 spacetime. In natural units, $\hbar = c = 1$, for the particle with the proper time τ, the action can be expressed as

$$\mathcal{A}[z_\mu, \dot{z}_\mu] = m \int_{\tau_1}^{\tau_2} (-\dot{u}^2 - 2\dot{u}\dot{r} + r^2\dot{\varphi}^2)^{\frac{1}{2}} d\tau, \tag{4}$$

where z_μ is a typical coordinate and its velocity is given by $\dot{z}_\mu = \frac{dz_\mu}{d\tau}$. The corresponding Lagrangian for our test particle is

$$L = m(-\dot{u}^2 - 2\dot{u}\dot{r} + r^2\dot{\varphi}^2)^{\frac{1}{2}}. \tag{5}$$

This Lagrangian is first-order in terms of velocity and belongs to a singular model, meaning that its phase space does not necessarily possess a symplectic structure, complicating its quantization. The system is inherently constrained to be first class. As a result, the quantization process will not be straightforward, and the corresponding quantum mechanics of the particle is expected to reveal novel physical properties that we aim to explore.

Taking the first step toward finding new physical properties, we calculate the corresponding momenta,

$$p = \frac{-m^2\dot{u}}{L}, \qquad h = \frac{-m^2}{L}, \qquad l = \frac{m^2 r^2 \dot{\varphi}}{L}. \tag{6}$$

Here, h is the canonical momentum corresponding to the time-like coordinate u, while p and l are the spatial coordinates, i.e., length and the angular dimensionless quantities. Given that the system has a single first-class constraint, this is a gauge model. This becomes evident when selecting the gauge $t = u + r$, which leads to the following primary constraint in configuration space

$$\dot{u} + \dot{r} = 1, \tag{7}$$

acting as a first-class identity, indicating the existence of gauge symmetry in the model.

The spacetime-invariant action is formulated such that its invariance directly reflects the underlying symmetry of spacetime. This symmetry can be understood through the gauge symmetries point of view, where assigning a specific coordinate to measure time (the transformation parameter) is effectively a form of gauge fixing.

In the Hamiltonian framework, the velocity relations can be solved using this constraint as follows:

$$\dot{u} = \frac{p}{h}, \qquad \dot{r} = \frac{h-p}{h}, \qquad \dot{\varphi} = \frac{-l}{r^2 h}. \tag{8}$$

The Legendre transformation gives the canonical Hamiltonian as

$$H_c = 2p - \frac{p^2 - m^2}{h} - \frac{l^2}{r^2 h}. \tag{9}$$

With the help of Equations (6) and (8), and the explicit form of Lagrangian (5), and by assuming $m \neq 0$ and the identity

$$L^2 = \frac{m^4}{h^2},$$

the phase space equivalent of the the primary constraint (7), previously represented in the configuration space as $H_c = 0$, defines a primary constraint,

$$\Phi = H_c. \tag{10}$$

Since h is the canonical conjugate of the time-like coordinate u, to solve h from the relation (10) in the quantized phase space, one should replace it with $i\partial_u$, while preserving the usual representations for p, l, r, and φ. Then, one should deal with the nonlinear wave equation,

$$i\partial_u \psi = \left(\frac{2p}{p^2 - m^2 + \frac{l^2}{r^2}} \right)^{-1} \psi, \tag{11}$$

and find the proper interpretations for ψ while getting rid of the non-physical parts of that. This is an arduous task since two parts of the Equation (11) do not commute [1]

$$i\partial_u \psi = \left(p\mathcal{A}^{-1} + \mathcal{A}^{-1} p \right) \psi, \qquad \text{with} \qquad \mathcal{A} = p^2 - m^2 + \frac{l^2}{r^2}. \tag{12}$$

Since the Hamiltonian function is not fully factorized in Equation (11), solving the eigenvalue equation

$$i\partial_u \psi = E\psi. \tag{13}$$

is not straightforward. To address this, we apply the gauge-fixing method and reduced phase space quantization, selecting a gauge orbit in the full phase space (not limited to the momentum space). By identifying the reduced phase subspace, we derive the canonical Hamiltonian and phase space structure of the model, ultimately finding the wave equation corresponding to the system's energy eigenvalues.

3. Reduced Phase Space Quantization

In this approach, we aim to minimize the effect of the gauge degrees of freedom, despite the inherent nonlinearity in our wave equation.

It is evident that the total Hamiltonian of the system,

$$H_T = (1 + \lambda)\Phi, \tag{14}$$

does not generate new constraints via the consistency of Φ, indicating that it is of the first-class type. Consequently, there exists a gauge degree of freedom in the complete set of phase space coordinates (r, φ, u, p, l, h). Rather than applying conventional gauge-fixing methods—which are not particularly useful in this context—we solve the constrained Equation (10) and derive a gauge-fixing condition for the deformed constraint

$$\tilde{\Phi} = h\Phi. \tag{15}$$

We have chosen the parameter h here, since (r, φ) and their corresponding momenta have the usual spatial and angular interpretation, whereas u is the evolution parameter of the system. The parameter h, in this case, aids in identifying the quantum operator form of the system's evolution function.

3.1. Fixing the Set (u, h)

Choosing the parameter u is a kind of clock regulation for the particle, which determines the Hamiltonian of the particle on the gauge orbit or one of the infinite copies of the reduced phase space. Hence, a straightforward gauge-fixing constraint is

$$\Phi_{gf} = u - at, \qquad 0 < a < 1, \tag{16}$$

which is the gauge that transforms the observer on the light cone (for $a = 0$) into a massive observer. To have a complete gauge fixing, this constraint should make a second class couple with $\tilde{\Phi}$, and determine the undetermined Lagrange coefficient in H_T.

$$\{\Phi_{gf}, \tilde{\Phi}\} = 2p, \qquad H_T = \frac{-1}{2p}\tilde{\Phi}. \tag{17}$$

In the physical space where $H_T \approx 0$, the Hamiltonian of the particle can be found from the relations (10) or (17). Consequently, the evolution parameter pair (u, h) can be expressed as

$$h = \frac{1}{2p}(p^2 - m^2 + \frac{l^2}{r^2}). \tag{18}$$

This means that there exists a Hamiltonian for the particle which is independent of the time evolution parameter, although it depends on the evolution parameter of the Minkowski observer via the definition of the BMS_3 time, according to the time of the Minkowski observer (1).

As can be observed, the Hamiltonian of the particle is defined over the entire phase space. However, the structure induced on the reduced subspace behaves like an antisymmetric metric, which is projected from the full phase space onto the reduced subspace along the selected gauge orbit via the condition Φ_{gf}. This structure, known as the symplectic structure, is obtained by calculating Dirac brackets—analogous to an induced metric—rather than Poisson brackets—similar to the metric of the entire space. The Dirac brackets are calculated between second-class constraints, which define the separation of the induced subspace from the full space, using the relation

$$\{A, B\}^* = \{A, B\} - \frac{1}{\Delta}\Big(\{A, \tilde{\Phi}\}\{B, \Phi_{gf}\} - \{A, \Phi_{gf}\}\{B, \tilde{\Phi}\}\Big), \tag{19}$$

where for the second class pair, we derive directly

$$\Delta = -2p. \tag{20}$$

This is the part where the ex-canonical couple (u, h) is distinguished from others as the evolution parameters and the factor determining the evolution of the Hamiltonian of the particle. The Dirac bracket of u with other phase space variables (or functions of them) vanishes, as does the constraint $\tilde{\Phi}$, since u is part of the second-class constraint. Therefore, the non-vanishing Dirac brackets of h with other principal variables are

$$\{r, h\}^* = 1 - \frac{h}{p}, \qquad \{p, h\}^* = \frac{-l^2}{pr^3}, \qquad \{\varphi, h\}^* = \frac{l}{pr^2}. \tag{21}$$

These relations can also be derived from the reduced symplectic phase space structure of (r, p, φ, l),

$$d\Omega = dr \otimes dp + d\varphi \otimes dl, \tag{22}$$

using the Jacobi and Leibniz identities, which remain valid for Dirac brackets. The symplectic structure in Equation (22), interpreted as the reduced phase space structure on (22), which is clarified as the reduced phase space structure on BMS_3 or the metric of that space, reveals that both the full space and its spatial component (r, φ) is not curved. In other words, the particle quantization on the BMS_3 is the quantization over a flat space, i.e., the coordinate part (r, φ)), with no intrinsic curvature, and only the Hamiltonian of the particle is in the form of (18). Dirac-quantized brackets (21) facilitate transforming the quantum wave equation of this model from a differential-integral equation—caused by the presence of $\frac{1}{p}$ in h—into a purely differential equation. Although an exact solution might not be readily attainable, it can be approached through approximation or iterative methods, as will be discussed in the following sections.

3.2. Quantization and Wave Equations

The quantized version of the model can be obtained by the Dirac procedure, using Dirac brackets. Having a Hamiltonian and some principal commutators,

$$\begin{aligned} h &= \frac{1}{4}\left(p^{-1}\mathcal{A} + \mathcal{A}p^{-1}\right), \\ [r,p] &= i, \qquad [\varphi, l] = i. \end{aligned} \tag{23}$$

The straightforward nature of this process lies in the standard form of the principal commutators, which dictates that the momentum operators in the spatial section follow the usual differential representations

$$p = -i\partial_r, \qquad l = -i\partial_\varphi. \tag{24}$$

However, the complexity arises from the presence of the inverse momentum operator in the Hamiltonian, preventing it from being represented by a finite number of principal operators.

From a mathematical standpoint, due to the differential representation of the momentum operator and the inclusion of both this operator and its inverse, the system's wave equation in relation (23) becomes a differential-integral equation. This equation can be addressed through approximation and iterative methods, using the quantum algebra of the principal variables and the Hamiltonian

$$\begin{aligned} [p,h] &= \frac{il^2}{2}(p^{-1}r^3 + r^3p^{-1}), \\ [r,h] &= i - \frac{i}{2}(hp^{-1} + p^{-1}h), \\ [\varphi,h] &= \frac{il}{2}(p^{-1}r^2 + r^2p^{-1}). \end{aligned} \tag{25}$$

The noncommutativity of the quantum operators A and h, due to (25), adds to the difficulty of the problem. In general, although finding the geodesics in the classical form seems to be easy and has exact solutions, finding geodesics in the quantum form is an arduous task.

Doing some algebra, we obtain the following iteration relations:

$$\begin{aligned} ph &= \frac{1}{4}(2\mathcal{A} + [p,\mathcal{A}]p^{-1}), \\ p^2h &= \frac{1}{4}(2p\mathcal{A} + [p,\mathcal{A}] + [p,[p,\mathcal{A}]]p^{-1}), \\ &\vdots \\ p^{n+1}h &= \frac{1}{4}(2p^n\mathcal{A} + p^{n-1}[p,\mathcal{A}] + \ldots + [p,[p,\ldots,[p,\mathcal{A}]\ldots]]p^{-1}). \end{aligned} \tag{26}$$

Similar to Baker–Hausdorff lemma expansion, there is no way to stop the expansion without having a kind of symmetry to make a commutator constant, which is not possible due to the form of the operator $\mathcal{A}$ in (23).

3.3. Ultra-Relativistic Limit

In this model, the parameter m simultaneously represents the mass, energy, and momentum scale. By multiplying the previous relations by the appropriate powers of m, it becomes evident that all terms on the right-hand side have matching factors of $\frac{p}{m}$ and $\frac{\mathcal{A}}{m^2}$, except for the last term, which includes an extra $\frac{p}{m}$ and, more significantly, an external factor of $\frac{m}{p}$ outside the quantum commutators.

In the ultra-relativistic limit, the presence of $\langle \frac{m}{p} \rangle \ll 1$ in the last term allows us to eliminate p^{-1}. Using this approximation, one can find the wave equations from the

Schrödinger equation $h\psi = E\psi$, which can be expressed in the following form to obtain the energy spectrum

$$p^n(h\psi)^{(n)} \cong \frac{1}{4}\Big(2p^{n-1}\mathcal{A} + p^{n-2}[p,\mathcal{A}] + ... + [p,[p,...[p,\mathcal{A}]...]\Big)\psi^{(n)} \tag{27}$$

The general form of the commutators in the right-hand side of the wave Equation (27) can be calculated as

$$[p,[p,...[p,[p,\mathcal{A}]]...]] = \frac{(n+1)!i^n l^2}{r^{n+2}}, \tag{28}$$

indicating that in the ultra-relativistic regime—when the particle is sufficiently far from the origin—the last term in Equation (26) becomes negligible.

Using (28), we can rewrite the $(n+1)$th term of the set of relations (26), while omitting the last term as

$$p^{n+1}h = \frac{1}{4}\left(2p^{n+2} - 2m^2p^n + p^n\frac{l^2}{r^2} + \sum_{n'=1}^{n} p^{n-n'}\frac{(n'+1)!i^{n'}l^2}{r^{n'+2}}\right). \tag{29}$$

Having the angular momentum operator l^2 and the corresponding quantum number j

$$l^2\psi = -\partial_\varphi^2\psi = j^2\psi, \qquad j \in \mathbb{Z}^+, \tag{30}$$

the $(n+1)$th order wave function can be read off as

$$2\psi_{(n+1)}^{(n+2)} - 4iE\psi_{(n+1)}^{(n+1)} + 2m^2\psi_{(n+1)}^{(n)} - j^2\left(\frac{1}{r^2}\psi_{(n+1)}\right)^{(n)} - j^2\sum_{n'=1}^{n}(n'+1)!\left(\frac{1}{r^{n'+2}}\psi_{(n+1)}\right)^{n-n'} = 0, \tag{31}$$

where the subscript index points to the order of the removed last term, and the superscript index is the order of derivative with respect to the radial variable r.

Now, we attempt to solve Equation (31) for small values of n to obtain the energy spectrum of the model. It is evident that the presence of the particle in BMS_3 has no impact on its energy spectrum, and E remains unchanged after quantization. The system, with a characteristic energy scale of m, has a continuous spectrum. As with other free systems, whether relativistic or nonrelativistic, the energy is not discretized unless a boundary condition, such as a finite length on the order of m^{-1}, is imposed. However, it should be noted that the system considered here does not include such a condition.

It is interesting to take a deeper look into the solutions for the cases with $m = 0$, which introduce a photon. In this scenario, the energy condition is similar to that in Minkowski coordinates, where $E = \pm\sqrt{\mathbf{p}^2 + m^2}$, but the dispersion relation (18) differs due to the inclusion of the factor r^{-1}.

$$E = \frac{1}{2p}\left(p^2 - m^2 + \frac{l^2}{\partial_p^2}\right). \tag{32}$$

The exact case of $m = 0$ case is not of primary interest, as it represents the vanishing point of the model built from (4). Therefore, we will focus on the more interesting ultra-relativistic regime instead.

3.4. New Phase in Quantum Mechanics

In addition to the discretization of physical quantities, such as the energy of a quantum system, the emergence of new phases during the quantization process is an important feature worth investigating in greater detail. The influence of these phases on the wave behavior of the physical system can provide insight into the quantum nature of the model.

This is why we aim to determine whether the wave behavior of the particle in the BMS_3 background exhibits a new phase beyond the conventional e^{-iEt}.

One might ask whether it would be easier to write the wave equation in momentum space, avoiding the need to eliminate the operator $\frac{1}{p}$ in h. It should be noted, however, that the presence of the term $\frac{1}{r^2}$ in h complicates the calculations. Furthermore, based on the chosen gauge for u in Equation (16), the relation between this quantity in the BMS_3 coordinates and the common polar coordinates in the plane, transitioning to Minkowski space (i.e., proper time and polar coordinates in the spatial part), causes the wave function to have a spatially dependent phase in the BMS_3 background, taking the form e^{iEr}. This phase can be studied within the framework of the Berry phase in quantum mechanics [36]. In continuation, we will explore these effects by solving for specific values of n that appear in the fundamental Equation (31), derived in this paper.

3.5. Differential Form of the Wave Equations and Their Solutions

The general form of the solutions that satisfy the wave equation is obtained in relation (31). While these equations are not explicitly in the form of eigenvalue-eigenvector pairs for the energy or wave function of the system, both quantities still satisfy the conditions imposed by them. Furthermore, solving this set of equations provides the wave equation and the energy states of the system to the specified accuracy, as mentioned below in Equation (31).

For $n = 0$, and the ultra-relativistic condition for our particles $m \to 0$, Equation (31) simplifies to,

$$\psi''_{(1)} - 2iE\psi'_{(1)} + \left(m^2 - \frac{j^2}{r^2}\right)\psi_{(1)} = 0. \tag{33}$$

This linear differential equation has solutions in terms of known special functions—specifically, the first and second kinds of Bessel functions—depending on the model's conditions, such as whether the particle is at the origin or at infinity (the non-regular singularity). By definition $\bar{j} = \sqrt{j^2 + \frac{1}{4}}$ and $\mathrm{M} = \sqrt{E^2 + m^2}$, the general solution can be written as,

$$\psi_{(1)} = e^{iEr}\sqrt{r}\Big(c_1 J_{\bar{j}}(\mathrm{M}r) + c_2 Y_{\bar{j}}(\mathrm{M}r)\Big) \tag{34}$$

For the cases where $m = 0$ and $j = 0$, the absence of intrinsic features of m and extrinsic features of j indicates that neither is capable of confining the particle within a specific region of space. The wave function of the particle, whether well-behaved at the origin (in the case of J) or not (in the case of Y), remains non-normalizable over the entire space, implying that the particle is free. This behavior is well-known in 3-dimensional radial solutions, and we now observe that it also holds in BMS_3 spacetime, which consists of a 2-dimensional spatial component. In fact, neither mass nor rotation can confine a particle in this spacetime, and the particle's continuous spectrum is given by Equation (32).

Nevertheless, the absence of an IR length, which could be imposed as a boundary condition in the model, indicates a non-quantized energy spectrum. We observe that $\frac{1}{m}$ acts as a UV length scale, which quantizes the spectrum similarly to a free particle in a box but disrupts the existence of a BMS_3 symmetry boundary condition. Comparing this with the relativistic Dirac equation, we see that despite the inclusion of the UV length scale $\frac{1}{m}$, two distinct energy states-matter and antimatter-are still obtained. This discrepancy may be due to the incompleteness of the Hamiltonian factorization.

Now, we take the next step and calculate for $n = 1$. Given the real nature of the order, the argument (variable), and the Bessel function itself, it is evident that no additional phase will appear in the wave function. Therefore, this step in solving the quantum wave equation in the BMS_3 background is an approximation of the zeroth order, and only the energy dispersion relation in terms of momentum, as given by Equation (32), yields a new result. This result arises from the nonlocality in momentum space.

For the subsequent steps in finding solutions, previous results indicate that to observe more significant effects of a particle's presence in this background field, we must consider how the specific choice of BMS_3 coordinates and their singularities are physically meaningful. The term $\frac{l^2}{r^2}$ has a singularity at $r = 0$, but it is evident that this singularity is not fundamental, as it resembles the typical behavior associated with angular momentum. Analyzing relation (33) and its solutions confirms that the singularity at $r = 0$ is regular, while the asymptotic behavior shows that $r \to \infty$ is an irregular and fundamental singularity. This singularity cannot be resolved physically, except by introducing a cut-off, which, however, would break the symmetry of the BMS_3 framework.

Thus, to uncover more physical properties of the model, we examine the higher orders for $n = 1$ in Equation (31). The $n = 1$ step results in a third-order linear equation with complex variable coefficients, given by

$$\psi'''_{(2)} - 2iE\psi''_{(2)} + (m^2 - \frac{j^2}{r^2})\psi'_{(2)} + \frac{3j^2}{r^3}\psi_{(2)} = 0. \tag{35}$$

In Equation (33), there is a regular singularity at $r = 0$ and a fundamental singularity at $r \to \infty$. This indicates that the behavior of the solutions at these singular points remains unchanged, though they become more precise. From this perspective, no new physics is introduced compared to the previous set of solutions. However, the rate at which the solutions decay or grow near the regular singularity at $r \to 0$ may increase or decrease, while the fundamental nature of the singularity is preserved. Notably, no intrinsic fundamental length emerges in Equation (35) or in the other equations.

To gain a deeper understanding, we will solve Equation (35) using the Frobenius method. In this approach, we substitute the expansion $\psi = \sum_{\nu=0}^{\infty} a_\nu r^{\nu+\lambda}$ into Equation (35) and reduce the equation by exploiting the linear independence of the terms $r^{\nu+\lambda}$. This leads to a system of differential-algebraic equations in recursive form for the coefficients a_ν. Here, the λ values serve as a control for the rate of convergence or divergence of the solution at the singular points (particularly at $r = 0$). For the third-order differential Equation (35), in addition to the indicial equation and the recursive relation, two other equations will also be derived as follows:

$$\lambda(\lambda - 1)(\lambda - 2) - j^2(\lambda - 3) = 0, \tag{36}$$

$$-2iEa_0\lambda(\lambda - 1) + a_1\Big((\lambda + 1)\lambda(\lambda - 1) - j^2(\lambda - 2)\Big) = 0, \tag{37}$$

$$m^2 a_0\lambda + a_2\Big((\lambda + 2)(\lambda + 1)\lambda - j^2(\lambda - 1)\Big) - 2iEa_1(\lambda + 1)\lambda = 0, \tag{38}$$

$$a_{\nu+3} = \frac{-m^2(\nu + 1 + \lambda)a_{\nu+1} + 2iE(\nu + 1 + \lambda)(\nu + 2 + \lambda)a_{\nu+2}}{(\nu + 3 + \lambda)(\nu + 2 + \lambda)(\nu + 1 + \lambda) - j^2(\nu + \lambda)}, \qquad \nu = 0, 1, 2, \ldots \tag{39}$$

The indicial Equation (36) for $1 \leq j \leq 4$ has one real and two complex roots, as indicated in Table 1. One may note that sgn(D) is the discriminant sign of the qubic Equation (36), i.e.,

$$D = 4\Big(1 + 3j^2 - 24j^4 + j^6\Big).$$

Due to the interaction with the specific shape of the potential in the wave Equation (35) for $1 \leq j \leq 4$, an additional phase appears in the wave function near the origin, which is distinctive and unique to BMS_3. We consider this wave function to be associated with the near-origin region because its real part consists of positive values. If we aim to observe this behavior physically, we would need to configure a setup around that region. As a conjecture, we propose that although λ is introduced in the Frobenius method to define the behavior of the radial wave function, and $\psi = \sum_{\nu=0}^{\infty} a_\nu r^{\nu+\lambda}$ is a radial wave function, different values of λ can be decomposed into real and imaginary parts. The real part determines the convergence or divergence at the regular singularity ($r = 0$) and the irregular singularity ($r \to \infty$), while the imaginary part of λ contributes a local phase to the wave function, as follows:

$$e^{i\delta(r)} \sim e^{(-i\text{Im}(\lambda)\ln(mr))}, \tag{40}$$

In this case, the approximate iteration of the wave Equations (31) and the higher orders are closely related to the phase transition caused by the constant potential. This is achieved through the iterative phase shift using the Born approximation method, with Equation (27) resembling a Lippmann–Schwinger equation.

Table 1. This table demonstrates that in the regime governed by Equation (35) for $1 \leq j \leq 4$, in addition to the primary phase factor e^{iEr}, a secondary phase factor emerges, as described by Equation (40).

j	sgn (D)	Real Roots	Imaginarty Roots
0	$+$	$0, 1, 2$	-
1	$-$	-0.77	1.88 ± 0.59i
2	$-$	-1.80	2.40 ± 0.94i
3	$-$	-2.83	2.92 ± 1.01i
4	$-$	-3.86	3.43 ± 0.83i
5	$+$	$-4.87, 3.60, 4.28$	-
6	$+$	$-5.89, 3.26, 5.63$	-

In the quantum scattering problem with fixed and variable potentials, the phase transition is directly influenced by the potential and is calculated based on the potential, angular states, and related quantum numbers. The situation is similar in this two-dimensional relativistic problem. The key difference is that, unlike in the non-relativistic case, the potential and kinetic terms of the particle are not separated into distinct components. However, we know that the factor $\frac{m}{p}$ behaves like a dimensionless potential of the model, interacting multiplicatively with other terms, as seen in Equation (26). Another difference in this scattering scenario is that, in addition to the inseparability of the scattered potential and the kinetic part, the scattering (and the resulting phase transition) occurs only when $j \neq 0$. Specifically, for $j \geq 5$, the term $\frac{j^2}{m^2r^2}$ dominates the scattering potential. In the region where $j = 0$, no scattering takes place, unlike in non-relativistic quantum scattering, where scattering occurs even when $j = 0$. When $m = 0$, we encounter a fully ultra-relativistic scenario, for which the Born approximation is applied.

3.6. Distortion near Light-Cone in BMS_3

Solving the state, $m \to 0$, provides at least a general idea to solve Equations (36) to (39). From a physical point of view, it can reveal the dispersion or deformation of the light cone in BMS_3 due to quantization. It suffices to find the wave function and use it to calculate the mean of r. The relation $r = u$ is the equation of a light cone and we need to put $< r >= u$ instead of $E = \omega$. However, the solution of sets (36) to (39) in this photonic regime is a linear combination of hypergeometric functions.

$$a_{\nu+1} = \frac{a_0(2iE)^\nu(\lambda)_\nu(\lambda+1)_\nu}{\left(1+\lambda-d-\frac{1+j^2}{3d}\right)_\nu\left(1+\lambda+e^{i\frac{\pi}{3}}d+\frac{e^{-i\frac{\pi}{3}}(1+j^2)}{3d}\right)_\nu\left(1+\lambda+e^{-i\frac{\pi}{3}}d+\frac{e^{i\frac{\pi}{3}}(1+j^2)}{3d}\right)_\nu} \tag{41}$$

with $\nu = 0, 1, 2, \ldots$, and

$$d = 3^{-\frac{2}{3}}\left(\frac{1}{2}\sqrt{-3D}-9j^2\right)^{\frac{1}{3}}, \tag{42}$$

and D is the discriminant that is defined earlier, and $(a)_n$ is the usual Pochhammer symbol.

Although we solved the recurrence relation for $m \to 0$, the solution implies that at least E is not discretized, as suggested by the form of expression (41). However, the appearance of non-trivial phases in the wave function, and its dependence on the quantum number j, provide a crucial clue for an observer at position m to infer events related to a distant massive object.

While averaging might not yield a closed-form solution, it can still be computed numerically. A more precise approach could involve calculating the evolution of the operator r in the Heisenberg picture, as demonstrated in (21), which gives

$$\frac{dr^{(h)}}{du} = \frac{1}{i}\left(1 - \frac{1}{2}(hp^{-1} + p^{-1}h)\right), \tag{43}$$

In Ehrenfest form, it becomes

$$< \dot{r}^{(h)} >_u = -i - i < p^{-1} >_u E. \tag{44}$$

With negligence, we set the first term equal to 1 because the resulting wave functions from (41), or more generally from (36) to (39), are divergent at $r \to \infty$ and require an IR cut-off. To calculate the second term, after extracting the wave function with the help of coefficients (41), we convert it to the momentum by the Fourier transform, where p^{-1} will be just a number (its representation is p^{-1} itself), and by integrating, we obtain the solution. However, this holds true only if p^{-1} is considered in the Heisenberg picture. In this case, during the calculation of the integral, in addition to the series expansion of the wave function, the term $p^{-1} = e^{ihu}p^{-1}e^{-ihu}$ must be expanded using the Baker–Hausdorff lemma. We should also calculate the commutator $[p^{-1}, h]$ from (23). Thus, despite its simple appearance, calculating $< p^{-1(h)} >_u$ is not straightforward, even for the case $m = 0$. Hence, the approximations of the wave function obtained from (41) and the approximations obtained via the Baker–Hausdorff lemma will not directly yield $p^{-1(h)}$. Ultimately, the wave function, whose expansion coefficients around $r = 0$ are obtained from Equations (36) to (39), takes the form of closed hypergeometric functions. While many of these solutions exhibit regular behavior at $r = 0$, all diverge as $r \to \infty$, indicating non-renormalizability across the entire space.

The structure of Equations (36) to (39), particularly the recurrence relation in (39), along with the calculation of the first few coefficients, shows that the phase of the wave function arises from the solution of the indicial Equation (36) for specific values of j. As mentioned earlier in this section, at each level of the Born approximation, solving the indicial equation leads to complex roots. The real part of these roots governs the regular behavior of the wave function at $r = 0$, while the imaginary part introduces a phase to the wave function. When a complex number is a root of the indicial equation, its conjugate is also a root. Consequently, the presence of complex roots causes a degeneracy in the wave function, manifested as differing phases in the wave function. Although the phase angles occur in negative pairs, they are not necessarily equal. This degeneracy in the wave function, stemming from the diversity of complex λs, can be interpreted as the existence of spin in the model solutions.

Although this phase is directly related to both j and r, and the number of complex roots depends on j, the total number of distinct phases can be attributed to the appearance of spin in the wave function. This is because the factor $e^{ij\phi}$ in the wave function corresponds to the degree of freedom ϕ, while the term $r^{\mathrm{Re}(\lambda)} \sum_{\nu=0} r^{\nu} a_{\nu}$ represents the well-tuned, convergent radial part of the wave function at $r = 0$ and its divergent behavior as $r \to \infty$. The remaining part of the wave function can be linked to its internal degrees of freedom.

The direct dependence of the wave function (40) on j (as the quantum number of the operator $\hat{l}$) and r (as the quantum number of the operator $\hat{r}$) suggests an interaction between an unknown spin operator and known particle observables, manifested in the detection of this degeneracy (spin). This is analogous to the first discovery of spin in the Stern–Gerlach experiment, where a spatially varying magnetic field revealed spin as spatial quantization.

For higher orders of the Born approximation, as we observed for $n = 1$ in the previous section, each iteration yields a differential equation of the form (31). From our experience with the cases $n = 0$ and $n = 1$, we know that the energy spectrum remains unchanged at each order. What introduces a semi-potential term $\frac{m}{p}$ is the phase transition in the wave function, which can be determined by deriving the wave function through series expansion or the Frobenius method.

After converting the differential Equation (31) into a set of algebraic equations for the series expansion coefficients, the first equation in this set, corresponding to the vanishing of the coefficient $r^{\lambda-(n+2)}$, results in an indicial equation of degree $n + 2$. By the fundamental theorem of algebra, this equation has $n + 2$ complex roots for λ. These λ values, which depend on j, yield both real and complex roots. The real part of these roots governs the behavior of the wave function at the singular points $r = 0$ and $r \to \infty$. However, it is impossible for any values of λ to remove the singularity at $r \to \infty$, as it represents a fundamental singularity.

The imaginary part of λ introduces phases into the wave function, which can be attributed to the hard potential present in the Hamiltonian (18). Although this potential is not separable from the kinetic term, as in non-relativistic problems, it still influences the phase structure of the wave function.

According to the fundamental theorem of algebra, the indicial equation in the nth order of approximation has $n + 2$ roots, some of which are complex (in even numbers). In general, the total number of these roots is tied to the order of the Born approximation and, in particular, to the value of j. What is clear is that as the degree of approximation increases, the number of complex roots also increases. If, as mentioned, we associate this degeneracy of complex roots with the particle's spin in the model, then approaching higher orders of the Born approximation, i.e., as $n \to \infty$, predicts an infinite (but countable) spin for a particle within this background. The higher the approximation studied, the more components of this spin are uncovered. Notably, infinite spin is predicted even for near-photon particles in this model.

4. Concluding Remarks

In this paper, we explore the behavior of a particle with mass m in the background of BMS_3 symmetry induced by a distant massive object. Under this setup, the particle's quantum wave function satisfies the unique wave Equation (31). Analysis of this equation in the first-order approximation reveals that the particle's energy spectrum remains continuous, with no indication of mass quantization at this level. However, in the next order of approximation, although a full analysis of the wave equation and a discrete energy spectrum was not completed, Equations (34) and (39) suggest that, upon normalization of the wave function, energy quantization for the free particle does occur. This presents a potential way for experimental verification of the particle's effect on the BMS_3 background. These preliminary analyses indicate the need for a more detailed examination of the wave function.

A noteworthy feature in both approximation regimes is the emergence of two-phase factors, corresponding to the particle's energy and angular momentum as it orbits the distant massive object. Particularly intriguing is the phase associated with angular momentum, which may correspond to an internal degree of freedom, such as spin, in higher-order or more precise approximations. This suggests that further investigation of Equation (31) is needed to obtain a more complete particle spectrum and clarify the nature of these phase factors. By fully determining the particle spectrum and incorporating it into the scattering function, quantum statistical mechanics methods can be employed to explore the information carried by gravitational waves generated by the distant massive object. This could provide new insights into the quantum-gravitational interplay within the BMS_3 framework.

Author Contributions: Conceptualization: M.D., S.A.N. and M.M.; Data curation: M.D. and S.A.N.; Formal analysis: M.D., S.A.N. and M.M.; Investigation: M.D., S.A.N. and M.M.; Methodology: M.D.

and S.A.N.; Project administration: M.D.; Resources: M.D. and S.A.N.; Software: S.A.N.; Supervision: M.D.; Validation: M.D., S.A.N. and M.M.; Visualization: S.A.N.; Writing—original draft: S.A.N. and M.D.; Writing—review & editing: M.D., S.A.N. and M.M. All authors have read and agreed to the published version of the manuscript.

Funding: There is no acquisition of the financial support for the project leading to this publication.

Conflicts of Interest: Authors have no conflict of interest to declare.

Note

[1] Note: Equation (11) in the first attempt after quantization is written as a formal equation.

References

1. Oblak, B. *BMS Particles in Three Dimensions*; Springer International Publishing AG: Cham, Switzerland , 2017.
2. Bondi, H.; Burg, M.G.J.V.; Metzner, A.W.K. *Royal Society of London Proceedings*; Series A 269; The Royal Society: London, UK, 1962; pp. 21–52.
3. Sachs, R.K. *Proceedings of the Royal Society of London*; Series A 270; The Royal Society: London, UK, 1962; pp. 103–126.
4. Sachs, R.K. Asymptotic symmetries in gravitational theory. *Phys. Rev.* **1962**, *128*, 2851. [CrossRef]
5. Oblak, B. Thomas precession for dressed particles. *Class. Quant. Grav.* **2018**, *35*, 054001. [CrossRef]
6. Strominger, A. *Lectures on the Infrared Structure of Gravity and Gauge Theory*; Princeton University Press: Princeton, NJ, USA, 2018.
7. Barnich, G.; Compere, G. Classical central extension for asymptotic symmetries at null infinity in three spacetime dimensions. *Class. Quant. Grav.* **2007**, *24*, F15; Erratum in *IBID* **2007**, *24*, 3139 . [CrossRef]
8. Susskind, L. Holography in the flat space limit. *AIP Conf. Proc.* **1999**, *493*, 98.
9. Polchinski, J. S-Matrices from AdS Spacetime. *arXiv* **1999**, arXiv:hep-th/9901076. [CrossRef]
10. de Boer, J.; Solodukhin, S.N. A holographic reduction of Minkowski space–time. *Nucl. Phys.* **2003**, *B665*, 545. [CrossRef]
11. Solodukhin, S.N. Reconstructing Minkowski Space-Time. *arXiv* **2004**, arXiv:hep-th/0405252. [CrossRef]
12. Gary, M.; Giddings, S.B. Flat space S matrix from the AdS/CFT correspondence? *Phys. Rev D.* **2009**, *80*, 046008. [CrossRef]
13. Arcioni , G.; Dappiaggi, C. Holography in asymptotically flat spacetimes and the BMS group. *Class. Quant. Grav.* **2004**, *21*, 5655. [CrossRef]
14. Arcioni, G.; Dappiaggi, C. Exploring the holographic principle in asymptotically flat spacetimes via the BMS group. *Nucl. Phys. B* **2003**, *674*, 553. [CrossRef]
15. Barnich , G.; Troessaert, C. Symmetries of asymptotically flat four-dimensional spacetimes at null infinity revisited. *Phys. Rev. Lett.* **2010**, *105*, 111103. [CrossRef] [PubMed]
16. Barnich, G.; Troessaert, C. Aspects of the BMS/CFT correspondence. *JHEP* **2010**, *5*, 062. [CrossRef]
17. Barnich, G.; Troessaert, C. BMS charge algebra. *JHEP* **2011**, *12*, 105. [CrossRef]
18. Barnich, G.; Troessaert, C. Comments on holographic current algebras and asymptotically flat four dimensional spacetimes at null infinity. *JHEP* **2013**, *1311*, 003. [CrossRef]
19. Barnich , G.; Gomberoff, A.; Gonzalez, H.A. Flat limit of three dimensional asymptotically anti–de Sitter spacetimes. *Phys. Rev. D* **2012**, *86*, 024020. [CrossRef]
20. Barnich, G.; Gonzalez, A.G.H.A. Three-dimensional Bondi-Metzner-Sachs invariant two-dimensional field theories as the flat limit of Liouville theory. *Phys. Rev. D* **2013**, *87*, 124032. [CrossRef]
21. Barnich, G.; Gomberoff, A.; Gonzalez, H.A. Dual dynamics of three dimensional asymptotically flat Einstein gravity at null infinity. *JHEP* **2013**, *05*, 016. [CrossRef]
22. Barnich, G.; Troessaert, C. Finite BMS transformations. *JHEP* **2016**, *03*, 167. [CrossRef]
23. Barnich, G.; Donnay, L.; Matulich, J.; Troncoso, R. Super-BMS3 invariant boundary theory from three-dimensional flat supergr. *arXiv* **2015**, arXiv:1510.08824.
24. Barnich, G.; Oblak, B. Notes on the BMS group in three dimensions: I. Induced representations. *JHEP* **2014**, *1406*, 129. [CrossRef]
25. Barnich, G.; Oblak, B. Notes on the BMS group in three dimensions: II. Coadjoint representation. *JHEP* **2015**, *1503*, 033. [CrossRef]
26. Brown, J.D.; Henneaux, M. Central charges in the canonical realization of asymptotic symmetries: An example from three dimensional gravity. *Commun. Math. Phys.* **1986**, *104*, 207. [CrossRef]
27. Barnich, G.; Troessaert, C. Supertranslations call for superrotations. In Proceedings of the Workshop on Non Commutative Field Theory and Gravity, Corfu, Greece, 8–12 September 2010.
28. Abbott, L.F.; Deser, S. Stability of gravity with a cosmological constant. *Nucl. Phys. B* **1982**, *195*, 76. [CrossRef]
29. Abbott, L.F.; Deser, S. Charge definition in non-abelian gauge theories. *Phys. Lett. B* **1982**, *116*, 259. [CrossRef]
30. Deser, S.; Tekin, B. Energy in generic higher curvature gravity theories. *Phys. Rev. D* **2003**, *67*, 084009. [CrossRef]
31. Deser, S.; Tekin, B. Gravitational energy in quadratic-curvature gravities. *Phys. Rev. Lett.* **2002**, *89*, 101101. [CrossRef]
32. Hawking, S.W. DAMTP-2015-49. *arXiv* **2015**, arXiv:1509.01147. [CrossRef]
33. Blanchet, L.; Compère, G.; Faye, G.; Oliveri, R.; Seraj, A. Multipole expansion of gravitational waves: From harmonic to Bondi coordinates. *J. High Energ. Phys.* **2021**, *2021*, 29. [CrossRef]

34. Mädler, T.; Winicour, J. Bondi-sachs formalism. *Scholarpedia* **2016**, *11*, 33528. [CrossRef]
35. Hijano, E. Flat space physics from AdS/CFT. *JHEP* **2019**, *7*, 132. [CrossRef]
36. Berry, M.V. *Proceedings of Royal Society of London*; Series A 392; The Royal Society: London, UK, 1984; p. 45.